

Angular distributions of $N_2 (2\sigma_u)^{-1}$ photoelectrons including the effects of coupling to the $N_2 (3\sigma_g)^{-1}$ channel

Bryan Basden and Robert R. Lucchese

Department of Chemistry, Texas A&M University, College Station, Texas 77843

(Received 25 August 1986)

We have performed a fixed-nuclei two-state coupled-channel calculation for the photoionization of N_2 leading to the $(2\sigma_u)^{-1} B^2\Sigma_u^+$ and $(3\sigma_g)^{-1} X^2\Sigma_g^+$ states of N_2^+ , using the Padé-approximant \bar{C} -functional formalism. We have found quantitative agreement with vibrationally unresolved experimental data for the photoelectron asymmetry parameter. Of particular interest is the good agreement of the asymmetry parameter in the $(2\sigma_u)^{-1}$ channel in the photon energy range of 25–35 eV where there are strong channel-coupling effects due to the shape resonance in the $(3\sigma_g)^{-1}$ channel.

I. INTRODUCTION

The characterization of shape resonances in molecular photoionization has greatly increased our understanding of the photoionization process, opening the door to obtaining dynamical information about the electronic structure of molecules, and has contributed significantly to progress in the field of photoionization in the last decade.¹ Shape resonances indicate that the photoelectron is trapped in a quasibound state, from which it slowly decays carrying analytic information about the localized potential which held it. Recent experimental work of Southworth, Parr, Hardis, and Dehmer,² and theoretical work of Stephens and Dill³ on the photoionization of N_2 , show that channel coupling between the channels leading to the $(2\sigma_u)^{-1} B^2\Sigma_u^+$ and $(3\sigma_g)^{-1} X^2\Sigma_g^+$ states of N_2^+ strongly affects the photoelectron asymmetry parameter in the $(2\sigma_u)^{-1}$ channel. The channel coupling is especially important in the photon energy region where there is the $3\sigma_g \rightarrow k\sigma_u$ shape resonance in the $(3\sigma_g)^{-1}$ channel.^{2,3} This shape resonance is believed to be responsible for the discrepancy in the photoelectron asymmetry parameter at photon energies of 25–35 eV between previous single-channel theoretical calculations⁴ and experiment^{2,5-9} for the $(2\sigma_u)^{-1}$ channel of N_2^+ . The calculation of Stephens and Dill³ was successful in qualitatively predicting the energy dependence of the asymmetry parameter and gave impetus for a more quantitatively accurate calculation. In this paper, we report results of application of the Padé-approximant \bar{C} -functional method^{4,10-14} to the photoionization of N_2 . We find that, in contrast to earlier theoretical studies,³ this method gives quantitative agreement with vibrationally unresolved experimental data for the photoelectron asymmetry parameter of the $(2\sigma_u)^{-1}$ channel of N_2 .

II. COUPLED-CHANNEL SCATTERING EQUATIONS

The present calculation employs single center expansions⁴ in which the potential is described via the frozen-core coupled-channel approximation. The nuclei are held fixed, which is equivalent to the vibrationally unresolved

results obtained with the Franck-Condon approximation. As in the frozen-core Hartree-Fock calculations of Lucchese, Raseev, and McKoy,⁴ the target orbitals of the initial-state Hartree-Fock wave function are used unchanged in the final-state ionic target wave functions. In the multichannel case, the final-state wave function

$$\Psi_{cc} = \sum_n \Psi_{\mathbf{k}_n, t_n} \quad (1)$$

is a linear combination (n is the channel index) of spin-adapted Slater determinants

$$\Psi_{\mathbf{k}_n, t_n} = (2)^{-1/2} (|\phi_1 \alpha \phi_1 \beta \cdots \phi_{t_n} \alpha \phi_{t_n} \beta \cdots \phi_s \alpha \phi_s \beta| + |\phi_1 \alpha \phi_1 \beta \cdots \phi_{t_n} \alpha \phi_{t_n} \beta \cdots \phi_s \alpha \phi_s \beta|), \quad (2)$$

where the ionized electron is removed from orbital ϕ_{t_n} . The coupled-channel wave function satisfies the projected Schrödinger equation¹⁵

$$\left\langle \sum_m \delta \Psi_{\mathbf{k}_m, t_m} | H - E | \Psi_{cc} \right\rangle = 0, \quad (3)$$

where the electronic Hamiltonian in atomic units is

$$H = \sum_{i=1}^N f(i) + \sum_{\substack{i,j \\ (i < j)}} \frac{1}{r_{ij}}, \quad (4)$$

N is the number of electrons, with

$$f(i) = -\frac{1}{2} \nabla_i^2 - \sum_a \frac{Z_a}{r_{ia}}, \quad (5)$$

and where the $\delta \Psi_{\mathbf{k}_m, t_m}$ are all possible variations of $\Psi_{\mathbf{k}_m, t_m}$ which can be obtained by variations in the channel scattering functions $\phi_{\mathbf{k}_m, t_m}$. As was the case for the single-channel calculation,⁴ it can be shown that for the coupled-channel scattering equations for photoionization of closed-shell systems within the frozen-core approximation, the continuum channel functions can be assumed to be orthogonal to the target orbitals.¹⁶ Hence, from Eq. (3), the continuum wave function must satisfy

$$0 = \langle P \delta \phi_{\mathbf{k}_m, t_m} | H^{\text{HF}} - E_m - J_{t_m, t_m} + K_{t_m, t_m} | P \phi_{\mathbf{k}_m, t_m} \rangle + \sum_{\substack{m, n \\ (m \neq n)}} \langle P \delta \phi_{\mathbf{k}_m, t_m} | 2K_{t_m, t_m} - J_{t_m, t_m} | P \phi_{\mathbf{k}_n, t_n} \rangle, \quad (6)$$

where P , H^{HF} , $J_{l_n t_m}$, and $K_{l_n t_m}$ are defined by

$$P = 1 - \sum_{i=1}^s |\phi_i\rangle\langle\phi_i|, \quad (7)$$

where s is the number of spatial orbitals,

$$H^{\text{HF}} = f + \sum_{i=1}^s 2J_{ii} - K_{ii}, \quad (8)$$

$$\langle\phi|J_{l_n t_m}|\phi'\rangle = \left\langle\phi(1)\phi_{l_n}(2)\left|\frac{1}{r_{12}}\right|\phi'(1)\phi_{l_n}(2)\right\rangle, \quad (9)$$

and

$$\langle\phi|K_{l_n t_m}|\phi'\rangle = \left\langle\phi(1)\phi_{l_n}(2)\left|\frac{1}{r_{12}}\right|\phi_{l_n}(1)\phi'(2)\right\rangle. \quad (10)$$

Use of the Phillips-Kleinman pseudopotential^{4,17}

$$\mathbf{V}_Q = \mathbf{V} - \mathbf{LQ} - \mathbf{QL} + \mathbf{QLQ}, \quad (11)$$

where \mathbf{L} , \mathbf{Q} , and \mathbf{V} are defined by

$$(\mathbf{L})_{nm} = \left[-\frac{1}{2}\nabla^2 - \frac{1}{r} + E_m \right] \delta_{nm} + (\mathbf{V})_{nm}, \quad (12)$$

$$(\mathbf{Q})_{nm} = \left[\sum_i |\phi_i\rangle\langle\phi_i| \right] \delta_{nm}, \quad (13)$$

$$(\mathbf{V})_{nn} = -\sum_a \frac{Z_a}{r_{ia}} + \frac{1}{r} + \sum_{i=1}^s (2J_{ii} - K_{ii}) - J_{l_n t_n} + K_{l_n t_n}, \quad (14)$$

and

$$(\mathbf{V})_{nm} = -J_{l_n t_m} + 2K_{l_n t_m}, \quad (15)$$

allows Eq. (6) to be solved via the matrix Lippman-Schwinger equation¹¹

$$\underline{\phi}_E = \underline{\phi}_E^c + \mathbf{G}_c \mathbf{V}_Q \underline{\phi}_E, \quad (16)$$

where $\underline{\phi}_E$ and $\underline{\phi}_E^c$ are the vectors of channel solutions and channel Coulomb waves, and \mathbf{G}_c is the matrix of channel Coulomb Green's functions defined by

$$(\mathbf{G}_c)_{nm} = G_c(E_m) \delta_{nm}. \quad (17)$$

III. NUMERICAL TECHNIQUES

The multichannel \tilde{C} -functional approach with Padé-approximant corrections,¹⁰⁻¹⁴ was used in all reported calculations. Explicitly, the variational functional was

$$\begin{aligned} \mathbf{M}_{35}^3(\underline{\phi}_t, \underline{\phi}_E^c) = & \langle\underline{\phi}_t | \mathbf{r} | \underline{\phi}_E^c \rangle + \langle\underline{\phi}_t | \mathbf{r} \mathbf{G}_c \mathbf{V}_Q | \underline{\phi}_E^c \rangle + \langle\underline{\phi}_t | \mathbf{r} \mathbf{G}_c \mathbf{V}_Q \mathbf{G}_c \mathbf{V}_Q | \underline{\phi}_E^c \rangle \\ & + \sum_{\underline{\alpha}, \underline{\beta}} \langle\underline{\phi}_t | \mathbf{r} \mathbf{G}_c \mathbf{V}_Q \mathbf{G}_c \mathbf{V}_Q | \underline{\alpha} \rangle \langle \underline{\alpha} | \mathbf{V}_Q - \mathbf{V}_Q \mathbf{G}_c \mathbf{V}_Q | \underline{\beta} \rangle^{-1} \langle \underline{\beta} | \mathbf{V}_Q \mathbf{G}_c \mathbf{V}_Q | \underline{\phi}_E^c \rangle, \end{aligned} \quad (18)$$

where the $\underline{\alpha}, \underline{\beta}$ are elements of a multichannel scattering basis set. The initial variational result was corrected using the $[N/N]$ Padé-approximant approach,¹⁰ which was found to give convergence at all energies with $N \leq 3$. Channels included in the calculation were those leading to the $(2\sigma_u)^{-1} B^2\Sigma_u^+$ and $(3\sigma_g)^{-1} X^2\Sigma_g^+$ states of N_2^+ . The occupied orbitals of N_2 used as the target state wave functions were the same as in the single channel calculation.⁴ Values for the partial-wave expansion parameters¹² were as follows:

$l_m = 30$, maximum l included in the expansion of scattering functions.

$l_s^x = 30$, maximum l included in the expansion of the scattering functions in the exchange terms.

$l_i^x = (1\sigma_g)16; (2\sigma_g)10; (3\sigma_g)10; (1\sigma_u)15; (2\sigma_u)10; (1\pi_g)10$, maximum l included in the expansion of the occupied orbitals in the exchange terms.

$l_i^d = 30$, maximum l included in the expansion of the occupied orbitals in the direct potential.

$\lambda_m^x = 30$, maximum l included in the expansion of $1/r_{12}$ in the exchange terms.

$\lambda_m^d, \lambda_m^n = 60$, maximum l included in the expansion of $1/r_{12}$ in the direct potential and in the nuclear terms.

$l_p = 6$ for $3\sigma_g \rightarrow k\sigma_u$, 7 for $2\sigma_u \rightarrow k\sigma_g$, 6 for $3\sigma_g \rightarrow k\pi_u$, and 5 for $2\sigma_u \rightarrow k\pi_g$, maximum l included in the expansion of the scattering solution.

All functions with radial dependence were expanded on a grid of 800 points whose maximum extent was $r = 64.0$

a.u. The scattering basis set contained 28 Gaussian functions for $3\sigma_g \rightarrow k\sigma_u$, 22 for $2\sigma_u \rightarrow k\sigma_g$, 12 for $3\sigma_g \rightarrow k\pi_u$, and 12 for $2\sigma_u \rightarrow k\pi_g$. Further details are given elsewhere.¹⁶

IV. RESULTS

In Fig. 1 we compare the dipole length and velocity⁴ forms of the $(2\sigma_u)^{-1} N_2$ photoelectron asymmetry parameter with both vibrationally resolved² and unresolved^{6,9} experimental data. One possible explanation of the differences seen in Fig. 1 between the vibrationally resolved data of Southworth *et al.*² and the vibrationally unresolved data of Marr, Morton, Holmes, and McCoy⁵ and Adam, Morin, Lablanquie, and Nenner⁸ for photon energies at 25–35 eV is that there are strong non-Franck-Condon effects for this electronic transition. As has been discussed previously,^{18,19} the vibrationally resolved data for the $(3\sigma_g)^{-1}$ channel of N_2 show significant non-Franck-Condon behavior. This is due to the rapid variation of the electronic transition matrix element as a function of the internuclear separation in the region of the $3\sigma_g \rightarrow k\sigma_u$ shape resonance. One would then expect that channel coupling would also make these vibrational effects important in the $(2\sigma_u)^{-1}$ channel for photoelectron energies where there is a shape resonance in the $(3\sigma_g)^{-1}$ channel.^{2,3} The present fixed-nuclei calculations tend to confirm this explanation since very good agreement is found with the vibrationally

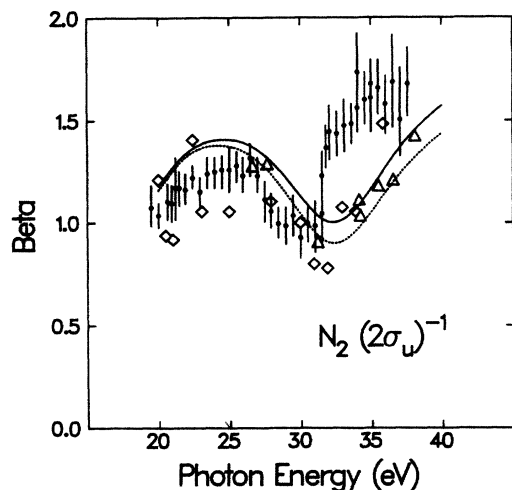


FIG. 1. Photoelectron asymmetry parameters for photoionization leading to the $(2\sigma_u)^{-1} B^2\Sigma_u^+$ state of N_2^+ : —, present results using the dipole-velocity approximation; ---, present results using the dipole-length approximation; ●, experimental results of Southworth *et al.* (Ref. 2); △, experimental results of Adam *et al.* (Ref. 8); ◇, experimental results of Marr *et al.* (Ref. 5).

unresolved data, although a vibrationally resolved calculation is needed to clarify this question. A comparison of various theoretical results is given in Fig. 2. In contrast to a single-channel exact Hartree-Fock⁴ result which contains no structure, the coupled-channel multiple scattering model (MSM) of Stephens and Dill³ qualitatively gives the effects of the shape resonance in the $(3\sigma_g)^{-1}$ channel on the $(2\sigma_u)^{-1}$ asymmetry parameters. However, as has been seen in many previous comparisons,^{4,12,19,20} the MSM

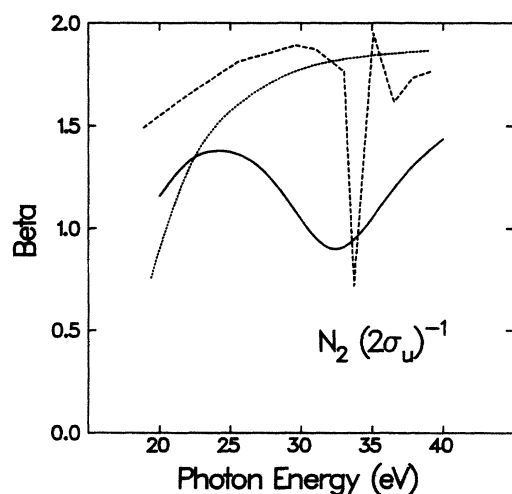


FIG. 2. Comparison of theoretical results for the photoelectron asymmetry parameter of photoionization leading to the $(2\sigma_u)^{-1} B^2\Sigma_u^+$ state of N_2^+ : —, present results using the dipole-length approximation; ---, theoretical results of Stephens *et al.* (Ref. 3); ····, exact Hartree-Fock results of Lucchese *et al.* (Ref. 4).

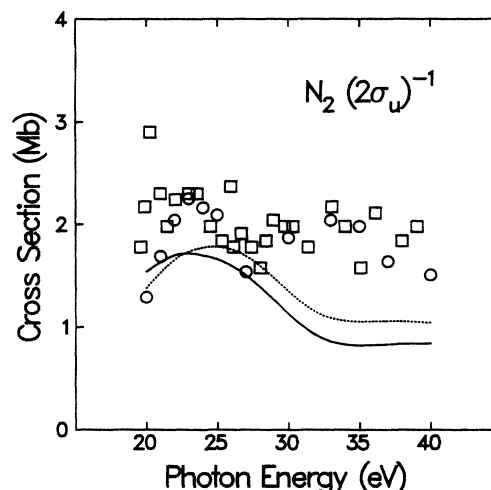


FIG. 3. Photoionization cross section of the channel leading to the $(2\sigma_u)^{-1} B^2\Sigma_u^+$ state of N_2^+ : —, present results using the dipole-velocity approximation; ---, present results using the dipole-length approximation; □, experimental results of Plummer *et al.* (Ref. 7); ○, experimental results of Hamnett *et al.* (Ref. 6).

approach gives much too narrow resonant features. In Fig. 3, we compare the $(2\sigma_u)^{-1}$ photoionization cross sections with experimental data. These cross sections are pushed down slightly compared to earlier single-channel results,⁴ but still give reasonable agreement with experiment.^{6,7}

V. CONCLUSIONS

We have found that an accurate two-channel photoionization calculation coupling the $(3\sigma_g)^{-1}$ and $(2\sigma_u)^{-1}$ channels in N_2 gives very good agreement with published vibrationally unresolved asymmetry parameters in the $(2\sigma_u)^{-1}$ channel. As was suggested by Stephens and Dill,³ the effects of the $3\sigma_g \rightarrow k\sigma_u$ shape resonance on the $(2\sigma_u)^{-1}$ channel have been found to be the main cause of the earlier disagreement between single-channel calculations and experimental data. Calculations are under way to examine the vibrational effects and the effects of coupling with the channel leading to the $(1\pi_u)^{-1} A^2\Pi_u$ state of N_2^+ on the cross sections and photoelectron angular distributions of the photoionization of N_2 .

ACKNOWLEDGMENTS

Acknowledgment is made to the Monsanto Company, the Dow Chemical Company Foundation, the Exxon Research and Engineering Company, and the Celanese Chemical Company for partial support of this research. In addition, this material is based upon work supported in part by the National Science Foundation under Grant No. CHE-8351414 and supported in part by the Robert A. Welch Foundation under Grant No. A-1020.

- ¹J. L. Dehmer, A. C. Parr, and S. H. Southworth, in *Handbook on Synchrotron Radiation*, edited by G. V. Marr (North-Holland, Amsterdam, 1986), Vol. II.
- ²S. H. Southworth, A. C. Parr, J. E. Hardis, and J. L. Dehmer, *Phys. Rev. A* **33**, 1020 (1986).
- ³J. A. Stephens and D. Dill, *Phys. Rev. A* **31**, 1968 (1985).
- ⁴R. R. Lucchese, G. Raseev, and V. McKoy, *Phys. Rev. A* **25**, 2572 (1982).
- ⁵G. V. Marr, J. M. Morton, R. M. Holmes, and D. G. McCoy, *J. Phys. B* **12**, 43 (1979).
- ⁶A. Hamnett, W. Stoll, and C. E. Brion, *J. Electron Spectrosc. Relat. Phenom.* **8**, 367 (1976).
- ⁷E. W. Plummer, T. Gustafsson, W. Gudat, and D. E. Eastman, *Phys. Rev. A* **15**, 2339 (1977).
- ⁸M. Y. Adam, P. Morin, P. Lablanquie, and I. Nenner, paper presented at International Workshop on Atomic and Molecular Photoionization, Fritz-Haber-Institut der Max-Planck-Gesellschaft, Berlin, West Germany, 1983 (unpublished).
- ⁹M. O. Krause, T. A. Carlson, and P. R. Woodruff, *Phys. Rev. A* **24**, 1374 (1981).
- ¹⁰R. R. Lucchese and V. McKoy, *Phys. Rev. A* **28**, 1382 (1983).
- ¹¹R. R. Lucchese, *Phys. Rev. A* **33**, 1626 (1986).
- ¹²R. R. Lucchese, K. Takatsuka, and V. McKoy, *Phys. Rep.* **131**, 149 (1986).
- ¹³M. T. Lee, K. Takatsuka, and V. McKoy, *J. Phys. B* **14**, 4115 (1981).
- ¹⁴K. Takatsuka and V. McKoy, *Phys. Rev. A* **23**, 2352 (1981).
- ¹⁵R. K. Nesbet, *Variational Methods in Electron-Atom Scattering Theory* (Plenum, New York, 1980), p. 9.
- ¹⁶B. Basden and R. R. Lucchese (unpublished).
- ¹⁷J. D. Weeks, A. Hazi, and S. A. Rice, in *Advances in Chemical Physics*, edited by I. Prigogine and S. A. Rice (Interscience, New York, 1969), Vol. XVI, p. 283.
- ¹⁸J. L. Dehmer, D. Dill, and S. Wallace, *Phys. Rev. Lett.* **43**, 1005 (1979).
- ¹⁹R. R. Lucchese and V. McKoy, *J. Phys. B* **14**, L629 (1981).
- ²⁰R. R. Lucchese and V. McKoy, *J. Phys. Chem.* **85**, 2166 (1981).